

1 **Modelling of deep adsorptive desulphurization of methanol for fuel cell** 2 **applications**

3 Eugeniusz Molga*, Robert Cherbański, Andrzej Stankiewicz, Michał Lewak

4
5 Chemical and Process Engineering Department, Warsaw University of Technology,
6 ul. Waryńskiego 1, 00-645 Warszawa, Poland
7

8 *Corresponding author, e-mail: eugeniusz.molga@pw.edu.pl
9

10 **Abstract**

11 These studies were carried out within the framework of the European FuelSOME Project (No.
12 101069828), which focuses on establishing a multi-fuel energy generation system based on
13 utilization of Solid Oxide Fuel Cells (SOFC) and is dedicated mainly to the long-distance
14 maritime shipping. For the SOFC stacks, the removal of sulphur contaminations from fuels is
15 crucial as the content of sulphur compounds is strictly limited, even to dozens of mol ppb.

16 The modelling and calculations were performed for a selected testing system of deep adsorptive
17 purification of methanol to remove dibenzothiophene (DBT) on activated carbon (AC), where
18 DBT was taken as a representative of compounds contaminating sulphur. An appropriate model
19 of the adsorption column packed with activated carbon pellets was elaborated as a basis for
20 process simulations and further techno-economic considerations. The research focused on
21 modelling sulphur removal to achieve the required purity of methanol, then on cost analysis to
22 optimize the proposed purification process. At the current stage, the aim of the performed
23 studies was a preliminary check of a possibility of successfully performing deep adsorptive
24 desulphurisation of methanol and an estimation of purification costs.

25 **Keywords:** methanol purification, sulphur removal, adsorber modelling, techno-economic
26 analysis, process optimization
27

This article has been accepted for publication and undergone full peer review but has not been through the copyediting, typesetting, pagination and proofreading process which may lead to differences between this version and the version of record. Please cite this article as DOI: [10.24425/cpe.2024.149467](https://doi.org/10.24425/cpe.2024.149467).

Received: 29 April 2024 | Revised: 10 August 2024 | Accepted: 27 August 2024



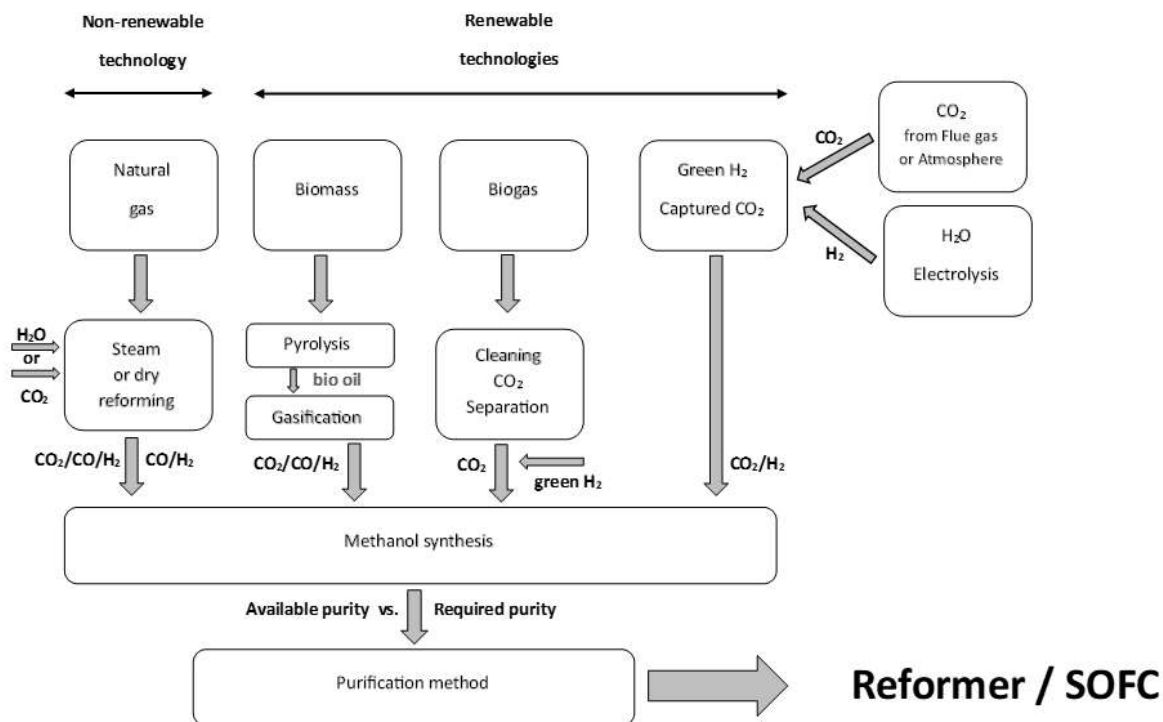
1. INTRODUCTION

28
29
30
31
32
33
34
35
36
37
38
39
40
41
42
43
44
45
46
47
48

Shipping is responsible for the annual emission of about 1 billion tons of carbon dioxide (CO₂) and about 2.5% of global anthropogenic greenhouse gas (GHG) emissions worldwide – e.g. see (CE Delft, 2019). Most ocean-going vessels operate using heavy fractions of petroleum, so GHG and air pollutants from ships, such as carbon dioxide (CO₂), nitrogen oxides (NO_x), sulphur oxides (SO_x) and particulate matters (PM), have to become key regulatory targets, in the EU and at a global level. The above issues are addressed, among other things, by the European FuelSOME project (FuelSOME, 2022). This project focuses on establishing the technological feasibility of a flexible, scalable, and multi-fuel capable energy generation system based on utilization of Solid Oxide Fuel Cells (SOFC) technology, specially dedicated to the long-distance maritime shipping.

Since hydrogen use on deep sea vessels is strongly limited due to difficulties of its storage and transportation, it is assumed that the proposed system should be able to operate mainly using ammonia and methanol. Therefore, the main challenge leading to the realization of such concept is to provide sufficient quantity of fuels, which meet strong quality requirements specific for the SOFC system.

Considering methanol as a very promising on-board fuel for fuel cell-powered vehicles and ships, the feedstocks and its production methods should be taken into account and evaluated. A schematic diagram to summarize methods for production of methanol as a fuel for SOFC applications is shown in Fig. 1, where the non-renewable and renewable pathways are distinguished.



49
 50 Figure 1. Schematic diagram to illustrate production and utilization of methanol as a fuel for
 51 SOFC.

52
 53 Different aspects of methanol use as an energy carrier are discussed in great detail in a review
 54 by Araya et al., 2020, where special attention is paid to renewable production methods.

55 In the literature of subject plenty of reports on methanol specifications can be found - e.g. see
 56 (Marcus and Glinberg, 1985). However, in the current times it is good to rely on regularly
 57 updated recommendations of the Methanol Institute (Methanol Institute, 2024), where it is
 58 stated that methanol is typically produced to meet the methanol specifications of the
 59 International Methanol Producers and Consumers Association (IMPCA). The current IMPCA
 60 Methanol Reference Specifications, updated in July 2021, can be found on the IMPCA website
 61 (IMPCA, 2024), where as many as 18 specifications are characterized – i.e. a given physico-
 62 chemical property and/or acceptable concentration of any impurity is described quantitatively
 63 and also standardized analytical methods to determine this are indicated. These reference
 64 specifications are listed in Table 1.

65
 66 Table 1. Methanol reference specifications recommended by the International Methanol
 67 Producers and Consumers Association (IMPCA) – (IMPCA, 2024).

	Test	Unit	Limiting value	Analytical Method
1.	Appearance	•	Clear and free from suspended matter	IMPCA 003
2.	Purity on dry basis	% w/w	Min 99.85	IMPCA 001
3.	Acetone	mg/kg	Max 30	IMPCA 001
4.	Ethanol	mg/kg	Max 50	IMPCA 001
5.	Colour	Pt-Co	Max 5	ASTM D 1209
6.	Water	% w/w	Max 0.100	ASTM D 5386
7.	Distillation range at 760 mmHg	°C	Max 1.0	ASTM D 1078
8.	Specific gravity 20 °C	-	0.7910–0.7930	ASTM D 4052
9.	Potassium permanganate time test at 15 °C	minutes	Min 60	ASTM D 1363
10.	Chloride as Cl-	mg/kg	Max 0.5	IMPCA 002
11.	Sulphur	mg/kg	Max 0.5	ASTM D 3961 ASTM D 5453
12.	Water miscibility (hydrocarbons)	-	Pass test	ASTM D 1722
13.	Carbonisables	Pt-Co	Max 30	ASTM E 346
14.	Acidity as acetic acid	mg/kg	Max 30	ASTM D 1613
15.	Iron in solution	mg/kg	Max 0.10	ASTM E 394
16.	Non-volatile matter	mg/1000ml	Max 8	ASTM D 1353
17.	TMA	-	TMA test	ASTM E 346
18.	Aromatics	-	UV-scan	IMPCA 004

68
69 Comparing purity requirements for SOFC application to the indications given by the IMPCA
70 in Table 1 it should be expected that the majority of methanol on the market does not meet so
71 strong demands. This is because the sulphur content in methanol for SOFC applications is
72 limited by SOFC stack producers to even 30 mol-ppb (Elcogen, 2020), while the limiting
73 sulphur concentrations in methanol recommended by the IMPCA (see Table 1) is equal to 0.5
74 mg/kg, which is equivalent to 500 mol-ppb. Because of that methanol for SOFC applications
75 should be always carefully analysed and pretreated before using.

76
77 The choice of methanol purification method depends on its production technology as well as
78 on used feedstocks. Water is indicated as the main impurity of methanol, so from this point of
79 view and considering that methanol is a good solvent for electrolytes, a content of dissolved
80 salts in methanol becomes an important issue. Generally, electrolytes which are well soluble in
81 water, are with some exceptions also soluble in methanol. The solubilities of some salts of the
82 alkali metals in methanol are shown in Table 2.

83

84 Table 2. Molal solubilities in [mol/kg MeOH) of some salts of alkali metals in methanol at
85 25 °C (Marcus and Glinberg, 1985).

	F ⁻	Cl ⁻	Br ⁻	I ⁻	NO ₃ ⁻	CO ₃ ²⁻	SO ₄ ²⁻
Li⁺	0.0068	4.95	3.95	*vs	6.23	0.0075	0.0115
Na⁺	0.0055	0.240	1.56	4.17	0.345	0.0293	0.0008
K⁺	0.394	0.071	0.175	1.029	0.0376	0.447	3 10 ⁻⁵
Rb⁺		0.111					
Cs⁺		0.215			0.0121		

86 *vs – very soluble

87
88 A special question discussed in the literature is whether silica dissolves in methanol. Although
89 this is particularly important for flush column chromatography, it can be also relevant for
90 utilization of methanol as a fuel for SOFCs. The majority of literature sources confirm that
91 silica does dissolve in methanol, although the Biotage reports the opposite (Biotage, 2023).

92 The purity of purchased methanol is very important but because of subsequent operations – e.g.
93 transportation, storage, and fuelling, a more detailed analysis of the methanol fate on its way
94 from the manufacturer to the fuel cell stacks is necessary. Appropriate analytical methods
95 should be used to effectively estimate the purity of methanol at every stage of that way, but
96 particularly just before feeding to the SOFC stacks. These methods should be rapid, accurate
97 and easy to use.

98 The simplest way to check methanol purity is to measure its density, which can be used for
99 crude methanol to determine significant amounts of water present. Other methods for the
100 determination of water in methanol depend on its concentration.

101 For the determination of the residual impurities in methanol (down to ppm levels) gas
102 chromatography is the best for detection of organic impurities, while flameless atomic
103 absorption for heavy metals (Marcus and Glinberg, 1985). However, more complex methods –
104 such as HPLC, HPLC-UV-MS (Spingern et al., 1981) and SPE - solid phase extraction (Poole,
105 2003) can also be employed.

106 Regardless of methanol synthesis technology, the post-production treatment is fundamental for
107 obtaining a high purity methanol stream. In industrial and analytical practice methanol
108 purification processes usually include removal of water and organic impurities, production of
109 conductivity-grade solvent and removal of bases and heavy metals.

110 Distillation, which is an immanent element of methanol production, is widely employed and is
111 extensively described in the literature. Numerous articles and patents dedicated to this topic
112 focus on the effectiveness of purification process as well as the economic analysis, because

113 distillation consumes a significant amount of energy - e.g. see (Fiedler et al., 2002; Luis et al.,
114 2014; Moiola and Pellegrini, 2021; Montevecchi et al., 2024, Pinto, 1980; Rocha et al., 2017;
115 Villegas et al., 2015; Zhang et al., 2010).

116 In some special cases, e.g. when a specific impurity forms an azeotrope with the methanol, a
117 distillation can be coupled with another separation technique, such as pervaporation (Luis et
118 al., 2014; Villegas et al., 2015) or extraction (Gil et al., 2009; Graczova and Vavrusova, 2018)
119 to effectively improve the removal of that impurity.

120 Purification by distillation process can be effectively utilized at the methanol production plant
121 for massive streams of methanol and significant amounts of impurities. However, for the
122 removal of residual impurities to meet high purity requirements – e.g. those for fuel cells –
123 more sophisticated methods should be applied. These include adsorptive separation applied
124 either as simple adsorption in a column filled with the sorbent or as continuous simulated
125 moving bed chromatography (Lee et al., 2002; Wen et al., 2010). It should be pointed out that
126 methanol preconditioning by adsorption can be carried out only to reach strong SOFC
127 requirements, so it is reasonable only for removal of trace impurities.

128 Although, according to our knowledge, there are no publications on deep desulfurization of
129 methanol (including also adsorptive desulfurization), valuable indications for a similar process
130 can be found in a recent review paper by Saha et al., 2021. This paper is devoted to
131 desulphurization of petroleum fuels, although systematized information on adsorbents for
132 sulphur removal, process kinetics and thermodynamics as well as on process parameters help
133 to search for a proper solution also for methanol purification.

134 Additionally, considering a choice of methanol purification method it should be necessarily
135 considered that in the FuelsOME Project methanol is not directly fed to the SOFC stacks, but
136 it is first decomposed in the reformer. Therefore, methanol contamination by water is not
137 important if its content does not significantly influence the methanol reforming process.
138 However an influence of water present in the methanol on the adsorptive removal of
139 contaminants can be crucial for efficiency of purification process. Also, the presence of non-
140 volatile inorganic salts, silica and others is not relevant as long as they are not thermally
141 decomposed in the reformer and can be effectively removed from it.

142

143 In this paper deep adsorptive removal of sulphur from methanol for SOFC applications is
144 modelled and analysed to check the possibility of successful performance of this process as
145 well as to estimate purification costs.

2. MODELLING OF ADSORPTIVE SULPHUR REMOVAL FROM METHANOL

Purification of methanol by adsorption was investigated for the following testing system: methanol contaminated with dibenzothiophene (DBT) – activated carbon (AC). DBT was taken as a representative of compounds contaminating sulphur, while activated carbon was assumed as the sorbent, since it is very efficient in removal of sulphur compounds (Lee et al., 2002).

Modelling and further considerations were performed for deep adsorptive desulphurization process carried out in a cylindrical column packed with spherical particles of activated carbon. In general case, the mass balance for DBT adsorption carried out over a differential control volume (i.e. along the differential column length – Δz) consists of two balance equations written for the liquid and solid phase, respectively. These balance equations must take into account and describe all stage processes and phenomena occurring in the considered system – i.e. the convective and dispersive flow of liquid through the column bed, the mass transfer from bulk of liquid to sorbent grains, the diffusional transport in the pores of sorbent as well as the adsorption rate and adsorption equilibrium. All of this results in a quite complex set of model equations and therefore appropriate simplifications are usually sought.

Based on the statistical moment analysis - e.g. see (Schneider and Smith, 1968; Carbonell and McCoy, 1975; and Molga, 2009) – a quantitative estimation of significance of each stage process was possible. Using this statistical moment analysis a series of calculations was carried out for process parameters listed in Table 3 and the range of operating parameters indicated in Table 4. However, it should be pointed out that some simplifications were required to utilize this method of moments – e.g. the adsorption equilibrium was approximated with a linear dependence. It was found that a significance of each above mentioned component process depends strongly on the sorbent particle diameter and to a lesser extent on the liquid interstitial velocity. Usually the results obtained with the analysis of statistical moments supply valuable indications for simplification of the full model. However, in the considered case, due to a quite wide range of the considered process diameters, a contribution of each stage process changes significantly depending on the considered case. Therefore, to keep a model description consistent and clear, all stage processes should be taken into account. This can be realized formulating a full model of the considered process, which is given in the Appendix – see Eqs. (A1–A11).

178 Table 3. Model parameters for process carried out at $T = 25\text{ }^{\circ}\text{C}$.

Parameter	Value or relationship to calculate	Source
D_L [m ² /s]	$\varepsilon Pe_L = 0.20 + 0.011 Re^{0.48}$	(Chung and Wen, 1968)
k_f [m/s]	$j_D = 1.17 Re^{-0.415}$	(Sherwood et al., 1975)
D_i [m ² /s]	$2.1 \cdot 10^{-10}$	(Carbonell and McCoy, 1975)
K_L [m ³ /mol]	0.8036	(Wen et al., 2010)
q_m [mol/kg]	1.1236	(Wen et al., 2010)
$k_{1,ad}$ [1/s]	$0.82 \cdot 10^{-3}$	(Wen et al., 2010)

179
 180 Kinetic and equilibrium data of Wen (Wen et al., 2010) were here adopted despite the fact that
 181 they were determined for the other system, i.e. for the DBT – diesel fuel system, as according
 182 to our knowledge no data for the DBT-methanol adsorptive system are available. This was for
 183 preliminary estimations only, which have to be verified with the results of our own
 184 measurements carried out for the DBT-methanol system.

185 As the solution of the full model presented in the Appendix (Eqs. A1–A11) is a quite complex
 186 numerical task, the following simplification was introduced into this model – i.e. the radial
 187 distributions of concentrations $c_{DBT,p}$ and q_{DBT} was replaced by the volume average ones: $\overline{c_{DBT,p}}$
 188 and $\overline{q_{DBT}}$, respectively. With this concept the full model of process is significantly simplified,
 189 taking simultaneously into account all the mentioned above stage processes.

190
 191 Table 4. The range of process parameters and operating conditions, for which model
 192 calculations were carried out.

Column and bed configuration					Operating conditions		Methanol properties	
L	D_w	ε	ε_p	d_p	G	$c_{DBT,in}$	ρ_M	μ_M
[m]	[m]	[-]	[-]	[m]	[kg/h]	[mol/m ³]	[kg/m ³]	[Pa s]
5.0	0.1 ÷ 0.5	0.45	0.55	0.001 ÷ 0.010	10 ÷ 500	2.15 ÷ 64.50	792	$0.544 \cdot 10^{-3}$

193
 194 This simplified version reads now as follows:
 195 • DBT mass balance in the liquid flowing through the packed bed

$$196 D_L \frac{\partial^2 c_{DBT}}{\partial z^2} - u \frac{\partial c_{DBT}}{\partial z} - \frac{6(1-\varepsilon)}{\varepsilon d_p} K_{gl} (c_{DBT} - \overline{c_{DBT,p}}) = \frac{\partial c_{DBT}}{\partial t} \quad (1)$$

197 • DBT mass balance inside the sorbent particle

$$198 \varepsilon_p \frac{\partial \overline{c_{DBT,p}}}{\partial t} = \frac{6}{d_p} K_{gl} (c_{DBT} - \overline{c_{DBT,p}}) - (1 - \varepsilon_p) \rho_s \frac{\partial \overline{q_{DBT}}}{\partial t} \quad (2)$$

199 where K_{gl} is the global mass transfer coefficient representing both, external and internal, mass
 200 transfer resistances, which is defined as:

$$201 \quad \frac{1}{K_{gl}} = \frac{1}{k_f} + \frac{1}{k_i} \quad (3)$$

202 where k_f – is the external mass transfer coefficient, while k_i is the apparent mass transfer
 203 coefficient representing internal mass transfer resistances, which is calculated as:

$$204 \quad k_i = \frac{10D_i}{d_p} \quad (4)$$

205 The presented concept and the relationship of Eq. 4 was proposed originally by (Glueckauf,
 206 1955), then repeatedly checked and applied by numerous researchers to describe the adsorption
 207 processes carried out in the column – e.g. see (Constantino et al., 2015; Santacesaria et al.,
 208 1982; Silva et al., 2011).

209 The effective intraparticle diffusion coefficient D_i [m^2/s], appearing in Eq. 4 is calculated as:

$$210 \quad D_i = \frac{D_M \varepsilon_p}{\tau} \quad (5)$$

211 where D_M [m^2/s] is the molecular diffusion coefficient for DBT in the methanol, while τ [-] is
 212 the tortuosity factor and ε_p – sorbent particle porosity.

213 The rate of adsorption $\frac{\partial \overline{q_{DBT}}}{\partial t}$ appearing in Eq. 2 can be easily estimated assuming adsorption
 214 equilibrium, so applying the equilibrium equation of Eq. A5 it can be expressed in terms of the
 215 appropriate volume average concentration in liquid filling pores $\overline{c_{DBT,p}}$.

216 The set of model equations (Eqs. 1- 2) can be solved with the following initial conditions:

$$217 \quad c_{DBT}(z, 0) = 0 \quad (6)$$

$$218 \quad \overline{c_{DBT,p}}(z, 0) = 0 \quad (7)$$

219 together with the Danckwerts boundary conditions:

$$220 \quad u c_{DBT,in} = u c_{DBT} - D_L \frac{\partial c_{DBT}}{\partial z} \quad \text{at } z = 0 \text{ and at any time} \quad (8)$$

$$221 \quad \frac{\partial c_{DBT}}{\partial z} = 0 \quad \text{at } z = L \text{ and at any time} \quad (9)$$

222 The appropriate values of model parameters appearing in Eqs. (1-9) - D_L , k_f , D_i , K_L , q_m or the
 223 relationships to calculate them are given in Table 3.

224 Notice that the contamination of methanol (shown in Table 3 as the molar concentration $c_{DBT,in}$)
 225 is often expressed as the mass fraction $x_{DBT,in}$ [% wt.], which can be easily recalculated to the
 226 molar concentration following the relationship:

$$227 \quad c_{DBT,in} = \frac{x_{DBT,in} \rho_M}{100 M_{DBT}} \left[\frac{mol}{m^3} \right] \quad (10)$$

228

229 Heat effect due to the adsorption process was here neglected due to a small concentration of
 230 adsorbed compound. Therefore the heat balance equation was abandoned and adsorption
 231 process was assumed to proceed at the constant ambient temperature.

232
 233 Based on the elaborated model, a series of simulations was carried out for different column
 234 and bed configurations as well as different operating conditions. The aim of these investigations
 235 was to estimate how the column configuration – i.e. its length L and diameter D_w , the structure
 236 of packed bed – i.e adsorbent particle diameter d_p , bed porosity ε and particle porosity ε_p , as
 237 well as operating conditions – i.e. the methanol mass flowrate G and the inlet concentration of
 238 DBT $c_{DBT,in}$ influence the efficiency of the purification process. The range of process parameters
 239 and operating variables used to carry out model simulations are listed in Table 4, where a quite
 240 wide variability of them can be observed.

241 The results of simulations supply the DBT concentration profiles in the liquid flowing in the
 242 bed intraparticle space $c_{DBT}(z, t)$ and the average concentration in sorbent pores $\overline{c_{DBT,p}}(z, t)$,
 243 so also the average concentration of the adsorbed compound $\overline{q_{DBT}}(z, t)$. However, from the
 244 performance point of view the most important is the concentration c_{DBT} as it directly helps to
 245 estimate the process efficiency.

246 Although quite a long column is indicated in Table 4, it does not mean that so long column is
 247 proposed to carry out the considered purification process – it was done only to obtain the results
 248 for different column lengths with a single calculation run.

249

250 3. Results and discussion

251 The carried out simulations supplied the results to find an influence of operating conditions on
 252 the efficiency of purification process, so also to carry out optimization of this process.

253 Note that according to the specifications supplied by the SOFC stack producer (Elcogen, 2020),
 254 the maximum concentration of sulphur compounds in the fuel supplied to fuel cells cannot
 255 exceed 30 mol-ppb. This means that the maximum molar concentration of DBT in the methanol
 256 stream supplied to the fuel cell cannot be higher than:

$$257 \quad c_{DBT,adm} = \frac{n_{DBT}}{n_M} \frac{\rho_M}{M_M} = \frac{30}{10^9} \frac{\rho_M}{M_M} = 0.742 \cdot 10^{-3} \left[\frac{mol}{m^3} \right] \quad (11)$$

258 So, for any case the relation between values the admissible concentration of $c_{DBT,adm}$ and the
 259 inlet DBT concentration $c_{DBT,in}$ determines purification requirements, so also a necessary
 260 efficiency of the considered adsorptive purification process.

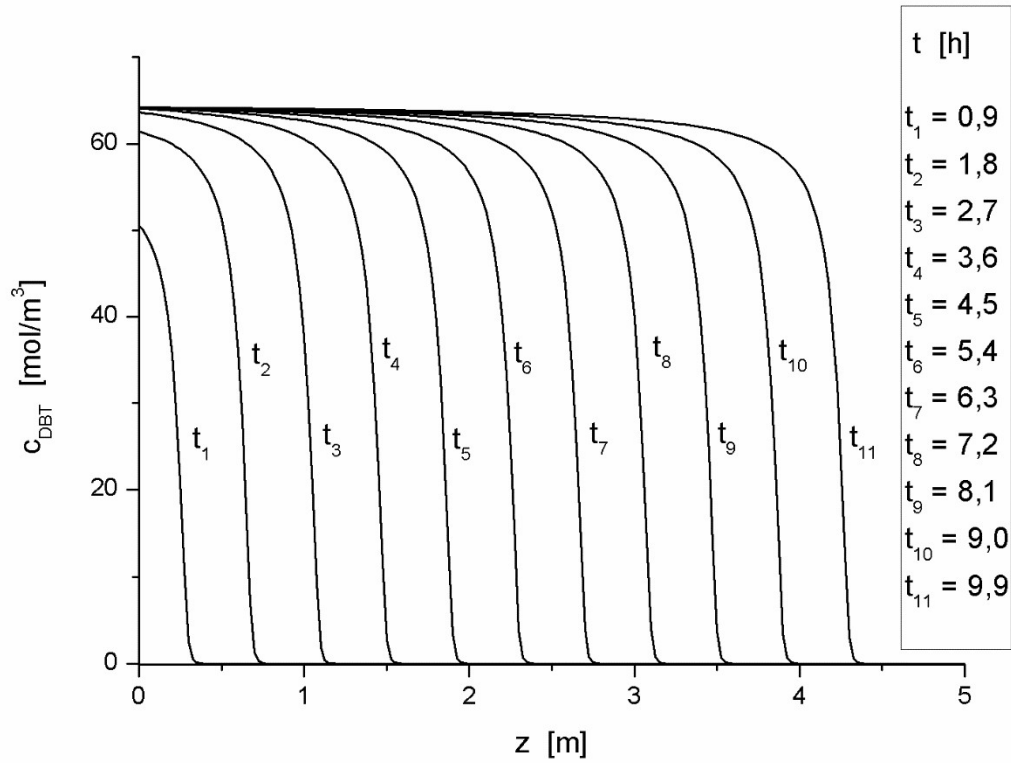
261

262 The set of model equations was implemented within the MATLAB environment and more than
263 30 series of simulations were performed for different combinations of the d_p , D_w , G and $c_{DBT,in}$
264 values.

265 Typical examples of the obtained results are shown as 2D diagrams in Fig. 2 and Fig. 3. In these
266 diagrams - for each chosen time moment - the DBT concentration profiles c_{DBT} are displayed
267 as a function of location along the adsorption column. In these figures it is clearly visible that
268 at the fixed axial location in the column after a specific time, called the breakthrough time, a
269 non-zero pollutant concentration in the liquid appears. Simultaneously, the zone where the
270 concentration of pollutant in the liquid phase became equal to the inlet concentration $c_{DBT,in}$
271 shifts gradually towards the column outlet – this is because of the saturation of the sorbent with
272 the adsorbed compound.

273 The characteristic feature of the investigated system can be observed in Figs. 2 and 3. Due to a
274 small concentration of pollutant in the purified methanol, the adsorption capacity of sorbent
275 placed in the column is relatively high, so to fully saturate sorbent bed the purification process
276 can be performed for a long time. This time becomes smaller while both, the inlet DBT
277 concentration $c_{DBT,in}$ and the methanol flow rate G decrease. In Figs. 2 and 3 two limiting cases
278 are shown – for the highest considered values of $c_{DBT,in}$ and G (Fig. 2) the column saturation
279 time is measured in dozens of hours, while for the lowest values of these operating parameters
280 (Fig. 3) the saturation time is as huge as even hundreds of days.

281



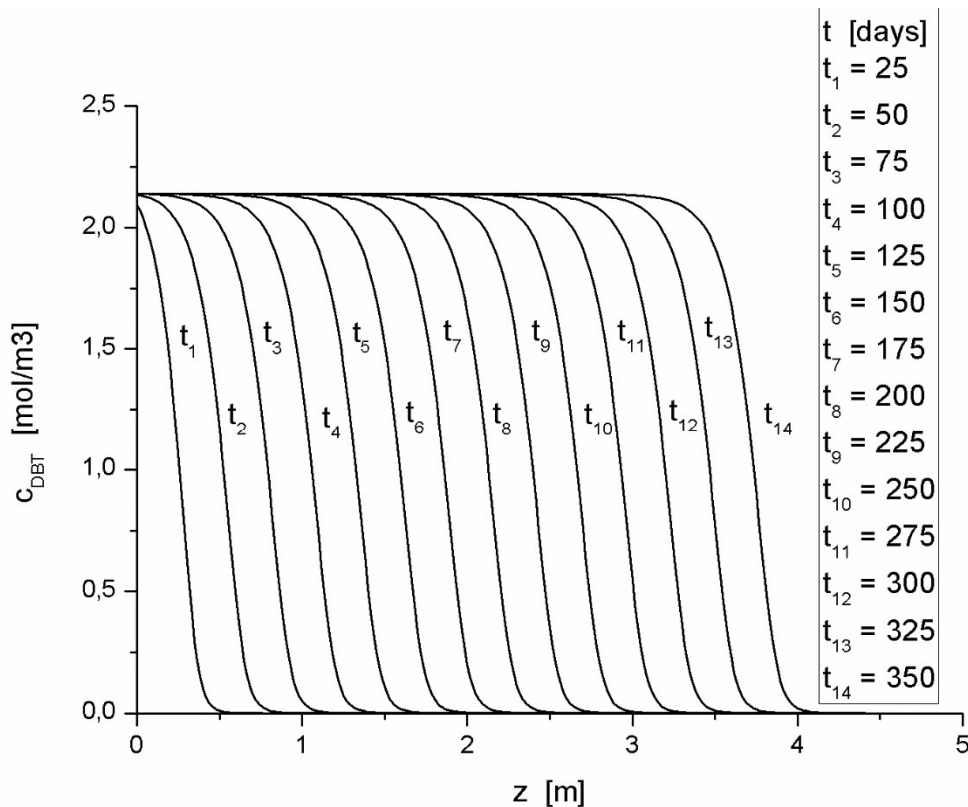
282

283 Figure 2. DBT concentrations in the liquid phase c_{DBT} as a function of the location in the
 284 adsorbent bed for indicated time moments. Process conditions: $c_{DBT,in} = 64.2$ [mol/m³]
 285 (equivalent to the weight percent $x_{DBT,in} = 1.5$ %), $D_w = 0.3$ [m], $d_p = 0.003$ [m], $G = 500$ [kg/h].

286

287 Due to a very high purity demand for methanol used to drive the SOFC stacks, a specific
 288 analysis of the considered purification process is proposed taking into account the limiting
 289 admissible concentration of sulphur compounds of 30 mol-ppb (equivalent to $0.742 \cdot 10^{-3}$
 290 mol/m³).

291



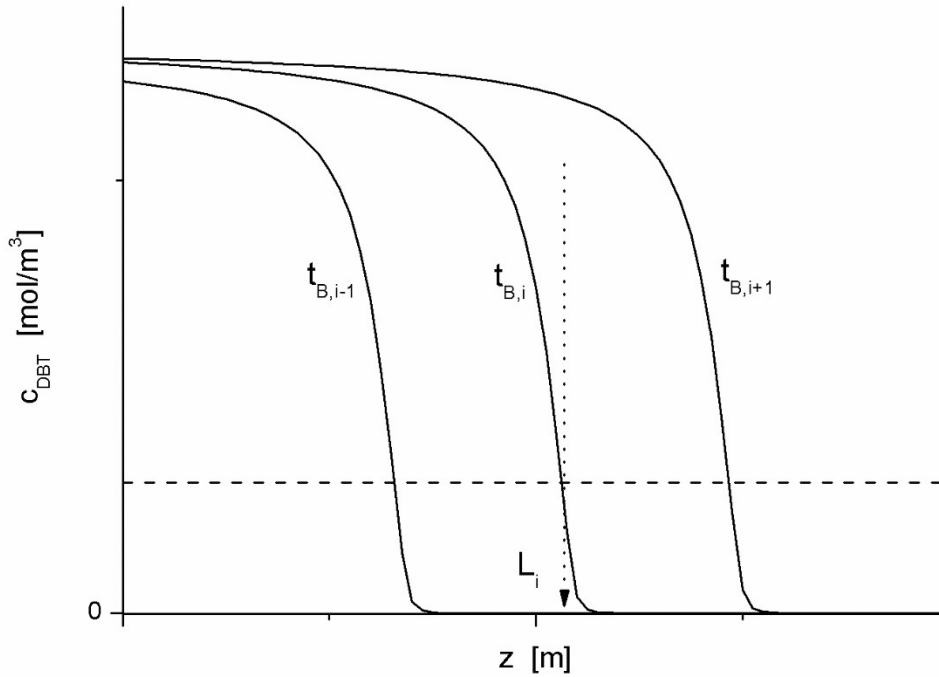
292

293 Figure 3. DBT concentrations in the liquid phase c_{DBT} as a function of the location in the
 294 adsorbent bed for indicated time moments. Process conditions: $c_{DBT,in} = 2.14$ [mol/m³]
 295 (equivalent to the weight percent $x_{DBT,in} = 0.05$ %), $D_w = 0.3$ [m], $d_p = 0.003$ [m], $G = 10$ [kg/h].

296

297 Such analysis helps to supply data for optimal design of the methanol purification process as
 298 well as for its cost evaluation. The proposed methodology is explained in Fig. 4, where the
 299 results obtained for any chosen calculation case are schematically shown. For each line,
 300 obtained for the time moment t , which describes a dependence of the DBT concentrations in
 301 the liquid phase vs. the bed length, the cross-point with the horizontal line indicating the
 302 admissible pollutant concentration ($c_{DBT,adm}$) can be found. This cross-point determines the
 303 breakthrough time – t_{Bi} (i.e. the time moment for which the DBT concentration in methanol
 304 reaches the admissible value) and the corresponding bed length – L_i . Both values (t_{Bi} and L_i)
 305 are crucial for assessment of the purification process performance. At chosen operating
 306 conditions for which the modelling was carried out, the fixed residence time - t_{Bi} (time of the
 307 column performance) sets the minimum bed length – L_i necessary to obtain the required
 308 methanol purity. However, a different approach can be also applied, when for the fixed column
 309 length – L_i the maximum necessary operating time - t_{Bi} can be found. In this case for times $t <$

310 t_{Bi} the outlet stream of methanol meets the purity requirements, while for times $t > t_{Bi}$
 311 concentration of the pollutant in the outlet stream exceeds this limiting value.
 312



313
 314 Figure 4. Determination of the dependence between the breakthrough time – t_{Bi} and the
 315 corresponding bed length – L_i .
 316

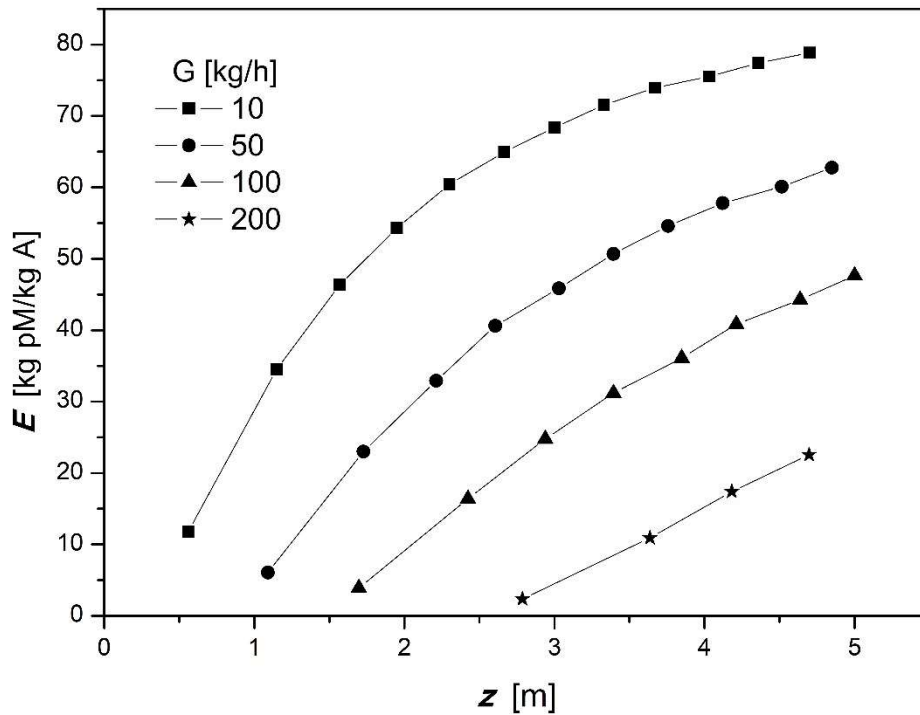
317 The described procedure was applied for all results obtained from simulations. The process
 318 efficiency factor E was introduced to present the results in a form suitable for designing the
 319 purification process. This factor is defined as the ratio of mass of the obtained purified methanol
 320 to the used sorbent mass as:

$$321 \quad E = \frac{m_{PM}}{m_A} = \frac{t_{B,i} G}{F_o L_i (1-\varepsilon) \rho_{S,a}} \quad (12)$$

322 where m_{PM} – is the mass of purified methanol obtained in a single purification run (from the
 323 beginning of the process till its stop after time $t_{B,i}$), m_A – mass of sorbent in the column, while
 324 $F_o = \pi D_w^2/4$ is the cross section area of the empty adsorption column.

325 Maximizing the value of factor E , the optimal operating conditions for the purification process
 326 can be found. In Fig. 5 an operating diagram for optimization the methanol purification is

327 presented, where a significant influence of the methanol mass flow rate G is clearly visible. An
 328 increase of the flow rate distinctly deteriorates the process efficiency.
 329



330
 331 Figure 5. Operating diagram to optimize methanol purification process - dependence of the
 332 efficiency factor E vs. the methanol mass flowrate G and the column length L_i . Process
 333 conditions - $c_{DBT,in} = 2.14$ [mol/m³] (equivalent to the weight mass fraction $x_{DBT,in} = 0.05$ %), D_w
 334 = 0.03 [m], $d_p = 0.003$ [m].

335
 336 From Fig. 5 it is also visible that the factor E increases with increase of the column length - L ,
 337 although the influence of the column length on total efficiency of purification process is more
 338 complex as the pressure drop in the bed, so also pumping costs, significantly depend on the
 339 adsorbent bed length. Because of this, the entire cost analysis should be carried out, which in a
 340 general case should contain the investment cost - C_I , as well as the operating cost - C_O .

341 The investment costs consist of the permanent part - C_{Ip} , which for any considered type of
 342 processing facility is almost constant as weakly depends on its size and configuration. The
 343 variable part of costs - C_{Iv} , significantly depends on the chosen configuration of purification
 344 plant. In turn, the operating costs - C_O contain here mainly methanol pumping costs - C_{OP} .

345 The components of costs listed above can be quantified as follows:

346 $C_{Iv} = \eta_L L_i + \eta_A m_A$ (13)

347 where η_L [€/m] is the unit investment cost of the adsorption column (cost for construction of
348 the column per 1 m of length), η_A [€/kg] unit cost of 1kg of adsorbent.

349 $C_{Op} = \eta_p \frac{\Delta P}{L} L_i Q t_{B,i}$ (14)

350 where η_p [€/J] is the unit cost of energy consumed for pumping, $\frac{\Delta P}{L}$ [Pa/m] - the specific
351 pressure drop in the adsorption column per unit length, Q [m³/s] – volumetric flow rate of
352 methanol through the adsorbent bed, where $Q = G/\rho_M$. Notice that the pumping costs - C_{Op}
353 estimated with Eq. 14, so also entire cost analysis, refer to a single purification run, which lasts
354 a period of time $t_{B,i}$.

355 The specific pressure drop in the adsorption column $\frac{\Delta P}{L}$ can be estimated with the Ergun
356 equation:

357 $\frac{\Delta p}{L} = 150 \frac{v_o \mu_M (1-\varepsilon)^2}{d_p^2 \varepsilon^3} + 1.75 \frac{v_o^2 (1-\varepsilon)}{d_p \varepsilon^3}$ (15)

358 where $v_o = \frac{4Q}{\pi D_w^2}$ is the superficial velocity of methanol in the adsorption column.

359 Finally the total cost of the considered methanol purification process, calculated for a single
360 purification run which lasts a period of time $t_{B,i}$, can be estimated as:

361 $C_T = a (C_{Ip} + C_{Iv}) t_{B,i} + C_{Op}$ (16)

362 where a [1/s] is the depreciation rate.

363 In search for the optimal performance of the considered purification process, the minimum of
364 the following functional dependency should be found:

365 $I = \frac{C_T}{m_{pM}} = \frac{c_T}{t_{B,i} G} = f(D_w, d_p, \varepsilon, G, x_{DBT,in})$ (17)

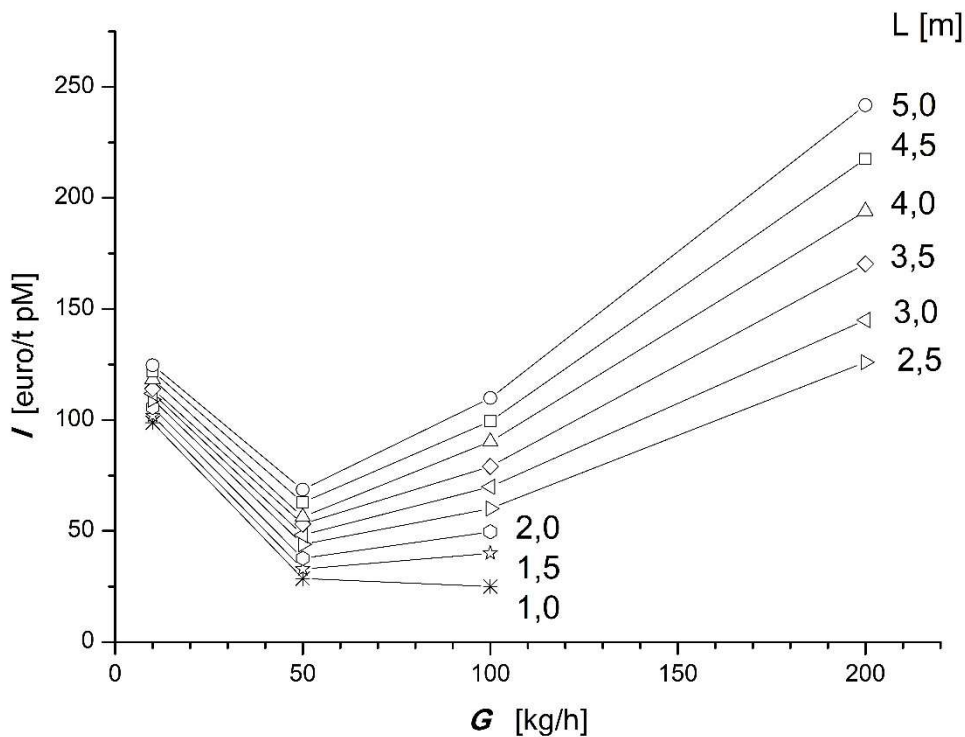
366 where I [€/kg] is the cost indicator determining the total cost of methanol purification per unit
367 mass of the purified product.

368 So, with use of the elaborated methodology, for any chosen column configuration (D_w, d_p, ε) as
369 well as operating conditions ($G, c_{DBT,in}$), the values of this cost indicator – I can be estimated.

370 The following values of cost parameters were assumed for calculations as a representative for
371 the considered case: $a = 1/5$ [1/years] = $6.34 \cdot 10^{-9}$ [1/s], $\eta_L = 40$ [€/m], $\eta_A = 10$ [€/kg], $\eta_p =$
372 0.4 [€/kWh] = $0.11 \cdot 10^{-6}$ [€/J]. These values should be treated only as indicative ones used to
373 demonstrate the proposed method as they can change depending on the year and the country.

374

375 An example of the proposed optimization procedure is shown in Fig. 6, where values of the
 376 indicator I are displayed vs. the methanol mass flowrate G . As is shown in this figure, for any
 377 chosen column and packed bed configuration (D_w, L, d_p, ε) and initial content of sulphur in the
 378 methanol ($c_{DBT,in}$) the minimum values of the cost indicator I (expressed here in € per ton of
 379 the purified methanol) can be found. For this value of I the optimal methanol mass flow rate
 380 G can be determined.
 381



382
 383 Figure 6. Determination of the optimum operating conditions for methanol purification process.
 384 Process conditions - $c_{DBT,in} = 2.14$ [mol/m³] (equivalent to the weight mass fraction $x_{DBT,in} = 0.05$
 385 %), $D_w = 0.03$ [m], $d_p = 0.003$ [m], $\varepsilon = 0.45$.

386
 387 A similar procedure was repeated for different column and bed configurations – i.e. different
 388 data sets of D_w, L, d_p, ε . It has been found that an increase of the sorbent particle diameter
 389 slightly deteriorates the sorption efficiency, although this effect is not very pronounced for total
 390 cost of process as due to lower pressure drop the pumping costs decrease. Notice that the
 391 proposed optimization procedure carried out in a multidimensional domain is a rather complex
 392 task, which requires advanced computational tools and skills. Because of this, the elaborated

393 procedure can be difficult for practical application – e.g. in a harbour, as for example the initial
394 content of sulphur ($c_{DBT,in}$) may change from batch to batch. Therefore, a smart and easy to use
395 method was developed. This is an expert system utilizing artificial neural networks (artificial
396 intelligence) which employs the results of performed simulations and techno-economic
397 analysis. The idea of this concept and the obtained results are presented elsewhere (Molga et
398 al., 2024).

399

400

4. SUMMARY

401 SOFC systems are very sensitive to the presence of sulphur, so purity requirements for used
402 fuels are very demanding. Typically, the content of sulphur compounds in the fuel-powered
403 SOFC stacks should be not higher than 30 ppb (Elcogen, 2020). According to the specifications
404 indicated for methanol producers by the IMPCA (Table 1) the admissible content of sulphur is
405 much higher than purity requirements defined for the SOFC fuel, therefore an efficient and deep
406 purification of this fuel is necessary. To meet such high purity requirements a deep adsorptive
407 purification method is here recommended and checked. In the performed study, a mathematical
408 model for this purification process was formulated. Based on the results obtained from
409 numerical simulations, the efficiency of the purification process was examined, then the
410 methodology to determine the optimal operating conditions elaborated and presented.
411 It was found that the application of deep adsorption for methanol purification enables efficient
412 preconditioning of this fuel to meet the very demanding purity requirements.

413

414

SYMBOLS

415

416	a	- depreciation rate, [1/year]
417	c_{DBT}	- DBT concentrations in the liquid phase in the interparticle space, [mol/m ³]
418	$c_{DBT,p}$	- DBT concentrations in the liquid phase in the sorbent pores, [mol/m ³]
419	$\overline{c_{DBT,p}}$	- volume average of the local $c_{DBT,p}$ concentration, [mol/m ³]
420	C_I	- investment cost, [€]
421	C_O	- operating cost, [€]
422	C_{Ip}	- permanent part of investment cost, [€]
423	C_{Iv}	- variable part of investment cost, [€]
424	C_{OP}	- operating costs (pumping cost), [€]
425	d_p	- adsorbent particle diameter, [m]

426	D_i	- effective intraparticle diffusion coefficient, [m ² /s]
427	D_L	- axial dispersion coefficient, [m ² /s]
428	D_M	- molar diffusion coefficient, [m ² /s]
429	D_w	- column inner diameter, [m]
430	E	- process efficiency factor, [kg _M / kg _A]
431	G	- liquid mass flowrate, [kg/h]
432	$I = C_T/(t_{B,i} G)$	- cost indicator, [€/kg]
433	$j_D = k_f/u Sc^{0.66}$	- factor for mass transfer, [-]
434	$k_{1,ad}$	- adsorption rate constant, [1/s]
435	K_L	- constant in the Langmuir equilibrium equation, [m ³ /mol]
436	L	- column length, [m]
437	$Pe = u d_p/D_L$	- Peclet number, [-]
438	q_{DBT}	- concentration of the adsorbed DBT in the solid phase, [mol/kg]
439	$\overline{q_{DBT}}$	- volume average of the local $q_{DBT,p}$ concentration, [mol/kg]
440	q_m	- constant in the Langmuir equilibrium equation, [mol/kg]
441	$Q = G/\rho_M$	- liquid volumetric flowrate, [m ³ /s]
442	$Re = (u \varepsilon d_p/\nu)$	- Reynolds number, [-]
443	$Sc = \nu/D_M$	- Schmidt number, [-]
444	t	- time, [s]
445	u	- liquid interstitial velocity in the bed, [m/s]
446	x_{DBT}	- mass fraction of pollutant, [% wt.]
447	z	- axial position, [m]
448		
449	$\frac{\Delta P}{L}$	- specific pressure drop in the adsorption column, [Pa/m]
450	ε	- bed porosity, [-]
451	η_L	- unit investment cost of the adsorption column, [€/kg]
452	η_A	- unit investment cost of the adsorbent, [€/kg]
453	η_p	- unit cost of energy consumed for pumping, [€/J]
454	μ_M	- methanol viscosity, [Pa s]
455	ρ_s	- density of adsorbent pellets, [kg/m ³]
456	ρ_M	- methanol density, [kg/m ³]
457		

458	<i>Subscripts and superscripts</i>	
459	adm	- admissible
460	A	- adsorbent
461	B	- breakthrough
462	eq	- equilibrium
463	in	- inlet
464	M	- methanol
465	PM	- purified methanol

466

467 *ACKNOWLEDGEMENTS*

468 This work is a part of the European Union’s Horizon Europe research and innovation program
 469 “FuelSOME” under Grant Agreement No. 101069828, funded by the European Union. Views
 470 and opinions expressed are, however, those of the authors only and do not necessarily reflect
 471 those of the European Union. Neither the European Union nor the granting authority can be
 472 held responsible for them.

473

474 REFERENCES

- 475 Araya S.S., Liso V., Cui X., Li N., Zhu J., Sahlin S.L., Jensen S.H., Nielsen M.P., Kaer S.K.,
 476 2020, A review of the methanol economy: the fuel cell route, *Energies*, 13, 596, 1-32. DOI:
 477 10.3390/en13030596.
- 478 Biotage, 2023, [https://www.biotage.com/blog/does-methanol-really-dissolve-silica-during-](https://www.biotage.com/blog/does-methanol-really-dissolve-silica-during-flash-column-chromatography)
 479 [flash-column-chromatography](https://www.biotage.com/blog/does-methanol-really-dissolve-silica-during-flash-column-chromatography), last check 18.04.2024
- 480 CE Delft, 2019, UMAS. Study on Methods and Considerations for the Determination of
 481 Greenhouse Gas Emission Reduction for International Shipping; Final Report Prepared for
 482 the European Commission; European Commission: Brussels, Belgium
- 483 Carbonell R.G., and McCoy B.J., 1975, Moment theory of chromatographic separation:
 484 resolution and optimization, *Chemical Engineering Journal*, 9, 115-124
- 485 Chung S.F., Wen C.Y., 1968. Longitudinal dispersion of liquid flowing through fixed and
 486 fluidized beds, *AIChE Journal*, 22, 1021-1032.
- 487 Constantino D.S.M., Pereira C.S.M, Faria R.P.V., Loureiro J.M., Rodrigues A.E., 2015,
 488 Simulated moving bed reactor for butyl acrylate synthesis: From pilot to industrial scale,
 489 *Chem. Eng. Processing*, 97, 153-168.
- 490 Elcogen, (2020). *Installation and operation manual of elcoStack® E3000 Version: 1.3.*

491 Fiedler E., Grossmann G., Kersebohm D. B., Weiss G., Witte, C., 2002, *Methanol. Ullmann's*
492 *Encyclopedia of Industrial Chemistry*, Wiley–VCH Verlag/GmbH & Co.

493 FuelSOME, 2022, Project number 101069828, HORIZON-CL5-2021-D2-01, Multifuel SOFC
494 system with Maritime Energy vectors, <https://fuelsome.eu/>

495 Gil I.D., Botla D.C., Ortiz P. and Sanchez O.F., 2009, Extractive distillation of
496 acetone/methanol mixture using water as entrainer, *Ind. Eng. Chem. Res.*, 48, 4558-4865.

497 Glueckauf E., 1955, Theory of chromatography, Part 10, Formula for diffusion into spheres and
498 their application to chromatography, *Trans. Faraday Soc.*, 51, 1540- 1551.

499 Graczova E. and Vavrusova M., 2018, Extractive distillation of acetone-methanol mixture using
500 1-ethyl, 3-methylimidazoliumtrifluoromethanesulfonate. *Chemical Engineering*
501 *Transactions*, 70, 1190-1194.

502 IMPCA Methanol Specifications, 2024, [http://www.impca.eu/IMPCA/Technical/IMPCA-](http://www.impca.eu/IMPCA/Technical/IMPCA-Documents)
503 [Documents](http://www.impca.eu/IMPCA/Technical/IMPCA-Documents), last check 8.04.2024

504 Lee S.H.D., Kumar R., Krumpelt M., 2002, Sulfur removal from diesel fuel-contaminated
505 methanol, *Separation and Purification Technology*, 26, 247-258.

506 Luis P., Amelio A., Vreysen S., Calabro V., and Van der Bruggen B., 2014, Simulation and
507 environmental evaluation of process design: Distillation vs. hybrid distillation–
508 pervaporation for methanol/tetrahydrofuran separation. *Applied Energy*, 113, 565-575.

509 Marcus, Y. and Glinberg S., 1985, Recommended method for the purification of solvents and
510 tests for impurities. Methanol and Ethanol, *Pure & Appl. Chem*, 57(6), 855-864.

511 Methanol Institute, <https://www.methanol.org/>, last check 8.04.2024

512 Moioli S. and Pellegrini L. A., 2021, Study of alternative configurations for methanol
513 purification, *Computer Aided Chemical Engineering*, 50, 267-272.

514 Molga E., 2009. *Procesy adsorpcji reaktywnej (Reactive adsorption processes)* (in Polish),
515 WNT, Warszawa, 90 -200.

516 Molga E., Chwojnowski K., Cherbański R., Stankiewicz A., 2024, Optimization of deep
517 adsorptive purification of methanol for fuel cells – use of expert system based on neural
518 networks application, Book of Abstracts, XII All-Polish Scientific Conference, Chemical
519 and Process Engineering for Environment and Medicine, Sarbinowo, 11-14.09.2024.

520 Montevecchi G., Cannio M., Cancelli U., Antonelli A., Romagnoli M., 2024, Evaluation of
521 distillery fractions in direct methanol fuel cells and screening of reaction products, *Clean*
522 *technologies*, 6, 513-527. DOI: 10.3390/cleantecnol6020027.

523 Pinto A., 1980, Methanol distillation process, US Patent 4, 210, 495.

524 Poole, C. F., 2003, New trends in solid-phase extraction, *Trends in Analytical Chemistry*, 22(6),
525 362-373.

526 Rocha L.B., Gimenes M.L., Faria S H.B., Jiménez L. and Cavali T., 2017, Design of a New
527 Sustainable Methanol Plant Coupled to an Ethanol Distillery. *Computer Aided Chemical*
528 *Engineering*, 40, 805-810.

529 Saha B., Vedachalam S., Dalai A.K., 2021, Review on recent advances in adsorptive
530 desulfurization, *Fuel Processing Technology*, 214, 106685, 1-21.

531 Santacesaria E., Morbidelli M., Servida A., Storti G., Carra S., 1982, Separation of Xylenes on
532 Y Zeolites. 2. Breakthrough curves and their interpretation, *Ind. Eng. Chem. Process*
533 *Des. Dev.*, 21, 446-451.

534 Schnieder P., Smith J.M., 1968. Adsorption Rate Constants from Chromatography, *AIChE*
535 *Journal*, 14, 762-771.

536 Sherwood T.K., Pigford R.L., Wilke C.R., 1975, *Mass Transfer*, McGraw-Hill, NY, 242.

537 Silva V.M.T.M., Pereira C.S.M., Rodrigues A.E., 2011, PermSMBR—A New Hybrid
538 Technology: Application on Green Solvent and Biofuel Production, *AIChE Journal*, 57,
539 1840-1851.

540 Spingern, N.E., Garvie-Gould, C.T., & Vuolo, L.L. ,1981, Analysis of methanol for reversed-
541 phase gradient elution liquid chromatography, *Anal. Chem*, 53, 565-566.

542 Villegas M., Vidaurre E.F.C. and Gottifredi J.C., 2015, Sorption and pervaporation of
543 methanol/water mixtures with poly(3-hydroxybutyrate) membranes, *Chemical*
544 *Engineering Research and Design*, 94, 254-265.

545 Wen, J., Han, X., Lin, H., Zheng, Y., Chu, W., 2010. A critical study on the adsorption of
546 heterocyclic sulfur and nitrogen compounds by activated carbon: Equilibrium, kinetics
547 and thermodynamics, *Chem. Eng. J.*, 164, 29-36. DOI: 10.1016/j.cej.2010.07.068.

548 Zhang J., Liang S., Fen X., 2010, A novel multi-effect methanol distillation process.
549 *Chemical Engineering and Processing Process Intensification*, 49, 1031-1037.

550

APPENDIX

551
552
553
554

The full model of the considered process of adsorptive purification of methanol consists of the following mass balance equations:

555 • DBT mass balance in the liquid flowing through the packed bed (in interparticle space)

$$556 \quad D_L \frac{\partial^2 c_{DBT}}{\partial z^2} - u \frac{\partial c_{DBT}}{\partial z} - \frac{6(1-\varepsilon)}{\varepsilon d_p} N_{DBT} = \frac{\partial c_{DBT}}{\partial t} \quad (A1)$$

557 where c_{DBT} [mol/m³] is the DBT concentration in methanol flowing through the packed bed (in
558 interparticle space), ε [-] - the bed porosity, u [m/s] - liquid interstitial velocity, D_L [m²/s] –
559 axial dispersion coefficient, d_p [m] – sorbent particle diameter, N_{DBT} [mol/m² s] – molar flux
560 for convective mass transfer from the liquid bulk to the sorbent grain surface, respectively.

561 • DBT mass balance inside the sorbent particle

$$562 \quad D_i \left(\frac{\partial^2 c_{DBT,p}}{\partial r^2} + \frac{2}{r} \frac{\partial c_{DBT,p}}{\partial r} \right) - \rho_s (1 - \varepsilon_p) \frac{\partial q_{DBT}}{\partial t} = \varepsilon_p \frac{\partial c_{DBT,p}}{\partial t} \quad (A2)$$

563 where $c_{DBT,p}$ [mol/m³] is the DBT concentration in methanol present in the sorbent pore space,
564 q_{DBT} [mol/kg] - concentrations of the adsorbed DBT, ε_p [-] – adsorbent pellets porosity, ρ_s
565 [kg/m³] – density of solid adsorbent. Notice, that Eq. (A2) was derived assuming application
566 of the pseudo-homogenous model, so D_i [m²/s] is the effective intraparticle diffusion
567 coefficient.

568 According to the used approach the concentration $c_{DBT} = f(z, t)$ depends on the axial location
569 in the adsorption column and the time, while the concentrations $c_{DBT,p} = g(z, r, t)$ and $q_{DBT,p} = h$
570 (z, r, t) depend additionally on the radial position in the sorbent grain.

571 The molar flux appearing in Eq. (A1) can be expressed as follows:

$$572 \quad N_{DBT} = k_f [c_{DBT} - c_{DBT,p}(r = R)] = D_i \left(\frac{\partial c_{DBT,p}}{\partial r} \right)_{r=R} \quad (A3)$$

573 where k_f [m/s] is the mass transfer coefficient. Eq. A3 is also formally the external boundary
574 condition, which binds the DBT concentrations outside (c_{DBT}) and inside ($c_{DBT,p}$) the sorbent
575 particle.

576 The adsorption rate – while assumed to be the first order - can be expressed as:

$$577 \quad \frac{d q_{DBT}}{dt} = k_{1,ad} (q_{DBT,eq} - q_{DBT}) \quad (A4)$$

578 where $k_{1,ad}$ [1/s] is the first order adsorption rate constant. The concentration $q_{DBT,eq}$ [mol/kg] is
579 the concentration of adsorbed DBT in equilibrium to the local DBT concentration in liquid
580 filling the pores ($c_{DBT,p}$), while q_{DBT} is just actual and local concentration of adsorbed DBT.

581 The equilibrium concentration $q_{DBT,eq}$ can be expressed in terms of the DBT pore concentration
582 $c_{DBT,p}$ according to the adsorption equilibrium equation. For Langmuir equation it reads as (Wen
583 et al., 2010):

$$584 \quad q_{DBT,eq} = \frac{q_m K_L c_{DBT,p}}{1 + K_L c_{DBT,p}} \quad (A5)$$

585

586 The set of model equations (Eqs. A1–A2) can be solved taking into account Eqs. (A3–A5) and
587 with the following initial conditions:

$$588 \quad c_{DBT}(z, 0) = 0 \quad (A6)$$

$$589 \quad c_{DBT,p}(z, 0) = 0 \quad (A7)$$

$$590 \quad q_{DBT}(z, 0) = 0 \quad (A8)$$

591 together with the following boundary conditions:

592 • the Danckwerts boundary conditions for the packed bed:

$$593 \quad u c_{DBT,in} = u c_{DBT} - D_L \frac{\partial c_{DBT}}{\partial z} \quad \text{at } z = 0 \text{ and at any time} \quad (A9)$$

$$594 \quad \frac{\partial c_{DBT}}{\partial z} = 0 \quad \text{at } z = L \text{ and at any time} \quad (A10)$$

595 • the symmetry condition in the adsorbent grain

$$596 \quad \frac{\partial c_{DBT,p}}{\partial r} = 0 \quad \text{at } r = 0 \quad (A11)$$

597